Steady bifurcations of higher multiplicity in pde2path

Hannes Uecker

Institut für Mathematik, Universität Oldenburg, D26111 Oldenburg
hannes.uecker@uni-oldenburg.de

April 30, 2018

Abstract

We describe the setup of systems of quadratic and cubic bifurcation equations for branch switching at steady bifurcation points of higher multiplicity in pde2path, with example applications to 2D and 3D pattern formation. The algorithms are designed for 2–and 3–determined problems, while for problems of higher order indeterminacy we additionally suggest some ad hoc methods.

1 Introduction

The Matlab continuation and bifurcation package pde2path [UWR14, Uec18c] can be used to numerically study solution branches and bifurcations in parameter dependent partial differential equations (PDEs). Typical examples are reaction diffusion systems of the form

$$\partial_t u = D\Delta u + f(u) =: -G(u,\lambda), \quad u = u(x,t) \in \mathbb{R}^N,\ t \geq 0,\ x \in \Omega, \tag{1}$$

where $\Omega \subset \mathbb{R}^d$ is a bounded domain, $d = 1, 2, 3$ (1D, 2D and 3D case, respectively), $D \in \mathbb{R}^{N\times N}$ is a positive (semi-)definite diffusion matrix, $\Delta = \partial^2_{x_1} + \ldots + \partial^2_{x_d}$, where the "reaction part" f is a smooth function, where λ in $G(u,\lambda)$ stands for parameters, and where (1) can be completed by various kinds of boundary conditions (BC). Typically, we have several parameters, and if (1) is extended by constraints, then several parameters become active, but we always have one *primary* parameter, and in the following we use λ in this scalar sense.

Given some steady solution u_0 at some parameter value λ_0, i.e.,

$$G(u_0, \lambda_0) = 0, \tag{2}$$

we want to continue this solution in the parameter λ, or, more generally, compute a branch $(u(s), \lambda(s))$ of solutions of (2) through (u_0, λ_0). In pde2path, this is done by a finite element discretization of (2) and arclength continuation [Kel77] in the discretized system, including the detection and localization of bifurcation points (BPs), where two or more branches intersect. Subsequently we can switch to a bifurcating branch of steady or time–periodic (Hopf) solutions, and this way can attempt to compute the bifurcation diagram for (1) and thus characterize the set of solutions in dependence of the parameters. See [Uec18c] for details on the class of systems pde2path can treat, its general setup, and download of tutorials and the software including various demo directories for model problems, and, e.g., [UW14, Uec16, Wet16, BGUY17, ZUFM17, Uec18a] for further examples, mostly related to Turing bifurcations [Tur52, Mur89], which means the bifurcation of spatially inhomogeneous solutions ("patterns") from a branch of spatially homogeneous solutions.

However, so far pde2path only dealt with *simple* BPs where exactly two solution branches intersect, although in applications (discrete) symmetries of the problem often force higher multiplicities of BPs. For instance, for Turing bifurcations over square domains with homogeneous Neumann BC we have "stripes in x_1" and "stripes in x_2" as two kernel vectors, and altogether we obtain three (modulo discrete spatial shifts) bifurcating branches, namely stripes (twice) and spots given by a superposition of the two stripes. In the following, we always use

$$m = \dim N(G_u(u_0, \lambda_0)) \tag{3}$$

to denote the dimension of the kernel of $G_u(u_0, \lambda_0)$, and call this m the *multiplicity of the BP* (u_0, λ_0).

The higher multiplicitity $m \geq 2$ of BPs in situations as above can be circumvented by some tricks. Essentially we can exploit the fact that even on ideal domains, the discretization breaks up multiple BPs, and/or we can strengthen this breakup by slightly distorting the domain. However, besides the lack of elegance, using these tricks has some serious disadvantages: (a) The localization of close together simple BPs (obtained from the breakup of multiple BPs) is quite inefficient. (b) The branching behaviour at the (artificially) simple BPs is in general quite different from that at the (original) multiple BP. For instance, two simple stripes may hide the spots also present. This then requires further tricks/analytical understanding to relate the numerics to the true analytical situation.

Thus, in this note we explain some new `pde2path` functions for branch switching at steady BPs of (in principle) arbitrary multiplicity $m \geq 2$. These 'automatic' branch switching functions are designed for so called 2–determined branches and 3–determined branches, but we also provide some fallback functions which (via additional user input) can be helpful for problems determined only at higher order. The problem of higher multiplicity Hopf bifurcations is considerably more complicated, see, e.g., [Kie79], and their treatment in `pde2path` will be given elsewhere.

In §2 we first briefly review some basics of arclength continuation and then explain our steady branch–switching algorithms. In §3 we apply them to the Swift–Hohenberg equation as a model problem. The associated demo directory `demos/sh` is included with the `pde2path` download at [Uec18c]. In §4 we conclude with comments on other `pde2path` demos, including a higher order indeterminate scalar problem on a hexagonal domain from [Mei00, §6.8.2]. More details and comments on the implementations of these demos and other problems of pattern formation in `pde2path` can be found in [Uec18b].

2 Numerical continuation and branch switching

Following [Kel77] we first recall some basics of arclength continuation, as for instance also implemented in AUTO [DCF+97] and MATCONT [DGK03]. Although much of the theory can be formulated in general Banach spaces X, in the following we let $X = \mathbb{R}^n$. The motivation is that `pde2path` uses finite elements to discretize (1) in space, which turns (1) into the (high–dimensional, i.e. typically n on the order of 10^4 to 10^5 in our applications) system of ordinary differential equations

$$M\frac{\mathrm{d}}{\mathrm{d}t}\mathrm{u} = -\mathrm{G}(\mathrm{u},\lambda) \tag{4}$$

for the nodal values $\mathrm{u} \in \mathbb{R}^n$, where $M \in \mathbb{R}^{n\times n}$ denotes the so called mass matrix. Similarly, the steady problem $G(u,\lambda) = 0$ turns into the algebraic problem

$$\mathrm{G}(\mathrm{u},\lambda) = 0. \tag{5}$$

For simplicity we henceforth drop the notational distinction between u and u, and G and G. When discussing eigenvalues/vectors μ, ϕ of the linearization $G_u(u_0,\lambda_0)$ at some (u_0,λ_0) we always refer to the generalized eigenvalue problem $\mu M\phi = -G_u(u_0,\lambda_0)\phi$, taking the mass matrix M on the left–hand side of (4) into account.

2.1 Basics

Consider a branch $(u(s),\lambda(s)) \in X \times \mathbb{R}$ of steady solutions of (5), parametrized by $s \in \mathbb{R}$, and let $(u_0,\lambda_0) = (u(s_0),\lambda(s_0))$ be a solution on this branch, i.e., $G(u_0,\lambda_0) = 0$. Arclength continuation works on extended system of the form

$$H(u,\lambda) = \begin{pmatrix} G(u,\lambda) \\ p(u,\lambda,s) \end{pmatrix} = \begin{pmatrix} 0 \\ 0 \end{pmatrix} \in \mathbb{R}^{n+1}, \tag{6}$$

where p is used to make s an approximation of arclength on the solution arc, typically

$$p(u,\lambda,s) := \left\langle \begin{pmatrix} u_0' \\ \lambda_0' \end{pmatrix}, \begin{pmatrix} u(s)-u_0 \\ \lambda(s)-\lambda_0 \end{pmatrix} \right\rangle_\xi - \mathrm{ds} = \xi \left\langle u_0', u(s)-u_0 \right\rangle + (1-\xi)\lambda_0'(\lambda(s)-\lambda_0) - \mathrm{ds}. \tag{7}$$

Here $\langle u, v\rangle$ is the standard inner product in $\mathbb{R}^n$, $\xi \in (0,1)$ is a weight, typically $\xi = \frac{1}{n}$, $\tau_0 := (u_0', \lambda_0') := \frac{\mathrm{d}}{\mathrm{d}s}(u(s), \lambda(s))|_{s=s_0}$ is a tangent to the branch, and $p(u,\lambda,s) = 0$ thus defines a hyperplane perpendicular (in the weighted scalar product) to τ_0 at distance $\mathrm{ds} := s - s_0$ from (u_0, λ_0). We may then use a predictor

$$\begin{pmatrix} u^1 \\ \lambda^1 \end{pmatrix} = \begin{pmatrix} u_0 \\ \lambda_0 \end{pmatrix} + \mathrm{ds} \begin{pmatrix} u_0' \\ \lambda_0' \end{pmatrix} \tag{8a}$$

for a solution (6) on that hyperplane, followed by a corrector using Newton's method in the form

$$\begin{pmatrix} u^{l+1} \\ \lambda^{l+1} \end{pmatrix} = \begin{pmatrix} u^l \\ \lambda^l \end{pmatrix} - \mathcal{A}(u^l, \lambda^l)^{-1} H(u^l, \lambda^l), \quad \text{where } \mathcal{A} = \begin{pmatrix} G_u & G_\lambda \\ \xi u_0' & (1-\xi)\lambda_0' \end{pmatrix}, \tag{8b}$$

and where $z = \mathcal{A}^{-1} b$ stands for the solution of the linear system $\mathcal{A} z = b$. Let (here and henceforth) $G_u^0 = G_u(u_0, \lambda_0)$ and $G_\lambda^0 = G_\lambda(u_0, \lambda_0)$. A point (u_0, λ_0) is called a regular point if G_u^0 is nonsingular; (u_0, λ_0) is called a fold point or normal limit point if

$$\dim N(G_u^0) = \mathrm{codim} R(G_u^0) = 1, \qquad G_\lambda^0 \notin R(G_u^0).$$

Differentiating $0 = G(u(s), \lambda(s))$ in s we obtain $0 = G_u u' + G_\lambda \lambda'$. At a fold point, applying $\langle \psi_0^T, \cdot \rangle$ with $N({G_u^0}^T) = \mathrm{span}\{\psi_0\}$ yields $0 = \left\langle {G_u^0}^T \psi_0, u_0' \right\rangle + \lambda_0' \left\langle \psi_0, G_\lambda^0 \right\rangle = \lambda_0' \left\langle \psi_0, G_\lambda^0 \right\rangle$, and using that $v \in R(G_u^0)$ if and only if $\langle \psi_0, v\rangle = 0$, and that $G_\lambda^0 \notin R(G_u^0)$, we obtain

$$\lambda_0' = 0 \text{ and } u_0' = \alpha \phi_0 \text{ for some } \alpha \neq 0. \tag{9}$$

Thus, the branch has a 'vertical' tangent, which explains the name fold. A fundamental result of arclength continuation, which inter alia yields that arclength continuation around folds is no problem, is as follows:

Theorem, [Kel77]. *Let (u_0, λ_0) be a regular point or a fold point, and let G be C^2 in some ball around (u_0, λ_0). Then there exists a unique smooth arc of solutions $(u, \lambda)(s)$ of (6) on $|s - s_0| \leq \rho$ for some $\rho > 0$, and on this arc $\mathcal{A} = \begin{pmatrix} G_u & G_\lambda \\ \xi u_0' & (1-\xi)\lambda_0' \end{pmatrix}$ is non-singular.*

2.2 Bifurcation points

A point (u_0, λ_0) is called a bifurcation point (BP) if two or more smooth branches intersect non-tangentially in (u_0, λ_0). (u_0, λ_0) is called a simple BP if exactly two branches intersect. There are two 'main' cases, which we briefly recall by way of scalar $(u, \lambda \in \mathbb{R})$ examples, i.e., $n = 1$ and hence naturally also the multiplicity of BPs $m = 1$:

(i) Transcritical bifurcation $G(u,\lambda) = u(\lambda - u)$. Trivial branch $u \equiv 0$, $\lambda \in \mathbb{R}$, nontrivial branch $(u(s), \lambda(s)) = (s, s)$, in particular $\lambda'(0) \neq 0$.

(ii) Pitchfork, $G(u,\lambda) = u(\lambda - u^2)$. Nontrivial branch $(u(s), \lambda(s)) = (s, s^2)$, $\lambda'(0) = 0$, $\lambda''(0) \neq 0$.

The pitchfork can be considered to be "non–generic" or "higher co–dimension", i.e., needs additional free parameter for the quadratic terms in u to vanish, but pitchforks naturally occur in problems with an up–down symmetry $u \mapsto -u$.[1] Further cases can occur, for instance:

(iii) Degenerate transcritical, $G(u,\lambda) = u(\lambda - u^3)$. Nontrivial branch $(u, \lambda) = (s, s^3)$, and thus $\lambda'(0) = \lambda''(0) = 0$, $\lambda'''(0) \neq 0$.

[1] Strictly speaking, the transcritical case is already non-generic because there are no constant terms, see e.g. [Kuz04].

(iv) Degenerate pitchfork, $G(u,\lambda) = u(\lambda - u^4)$. Nontrivial branch $(u,\lambda) = (s, s^4)$, $\lambda'(0) = \ldots = \lambda'''(0) = 0$, $\lambda''''(0) \neq 0$.

These are highly degenerate, but we shall see that a similar, i.e. more general, phenomenon of "high–order indeterminacy" can occur in problems with $m \geq 2$.

Our goal is to find numerically suitable branching equations for higher dimensional problems, $n \geq 2$ and typically large. Still following [Kel77], we first review the so called quadratic bifurcation equations (QBE), which generically will determine transcritical branches. By the above Theorem from [Kel77], and the Implicit Function Theorem, and since $G_u : \mathbb{R}^n \to \mathbb{R}^n$ is Fredholm of index 0, at a bifurcation point we have, for some multiplicity $m \geq 1$,

$$(a)\ \dim N(G_u^0) = \mathrm{codim} R(G_u^0) = m, \qquad (b)\ G_\lambda^0 \in R(G_u^0). \tag{10}$$

From (a) we have $N(G_u^0) = \mathrm{span}\{\phi_1, \ldots, \phi_m\}$, $N(G_u^{0T}) = \mathrm{span}\{\psi_1, \ldots, \psi_m\}$ with $\langle \phi_i, \psi_j \rangle = \delta_{ij}$, and by (b) there exists a unique $\phi_0 \in N(G_u^0)^\perp$ such that $G_u^0\phi_0 + G_\lambda^0 = 0$ and $\langle \phi_0, \psi_j \rangle = 0$, $j = 1, \ldots, m$. If $s \mapsto (u(s), \lambda(s))$ is any smooth branch with $(u,\lambda)(s_0) = (u_0, \lambda_0)$, then, since $G_u^0 u'(s_0) + G_\lambda^0 \lambda'(s_0) = 0$,

$$u'(s_0) = \sum_{j=0}^{m} \alpha_j \phi_j, \quad \alpha_0 = \lambda'(s_0), \tag{11}$$

where $\alpha_j = \langle \phi_j, \dot{u}(s_0) \rangle, 1 \leq j \leq m$. Moreover, by differentiating again,

$$G_u^0 u'' + G_\lambda^0 \lambda'' = -\big(G_{uu}^0[u', u'] + 2G_{u\lambda}^0 u'\lambda' + G_{\lambda\lambda}^0 \lambda'^2\big). \tag{12}$$

all evaluated at $s = s_0$. Since the left hand side is in $R(G_u^0)$, so is the right hand side, and applying $\langle \cdot, \psi_j \rangle$, $j = 1, \ldots, m$ yields a system of m *quadratic bifurcation equations (QBE)* for the $m+1$ coefficients $\{\alpha_0, \alpha_1, \ldots, \alpha_m\}$ (really m coefficients, because (13) is homogeneous, see below), namely

$$B(\alpha_0, \alpha) = 0 \in \mathbb{R}^m, \tag{13}$$
$$B_i(\alpha_0, \alpha) := \sum_{j=1}^{m}\sum_{k=1}^{m} a_{ijk}\alpha_j\alpha_k + 2\sum_{j=1}^{m} b_{ij}\alpha_j\alpha_0 + c_i\alpha_0^2, \quad 1 \leq i \leq m,$$
$$a_{ijk} = \left\langle \psi_i, G_{uu}^0[\phi_j, \phi_k] \right\rangle, \quad b_{ij} = \left\langle \psi_i, G_{uu}^0[\phi_0, \phi_j] + G_{u\lambda}^0\phi_j \right\rangle, \quad c_i = \left\langle \psi_i, G_{uu}^0[\phi_0, \phi_0] + 2G_{u\lambda}^0\phi_0 + G_{\lambda\lambda}^0 \right\rangle.$$

In summary, the tangent (u_0', λ_0') to any branch is of the form (11) with $\alpha_0, \alpha_1, \ldots, \alpha_m$ a solution of (13), unique up to a multiplicative constant γ. Thus, (13) gives a necessary condition to determine bifurcating branches. Conversely, each distinct *isolated* zero (α_0, α) gives a distinct solution branch of $G(u,\lambda)$ [KL72]. Here (α_0, α^*) is called isolated if for fixed α_0 and some $\delta > 0$ the only solution in $U_\delta^{\mathbb{R}^m}(\alpha^*)$ is α^*. By the implicit function theorem, a sufficient condition for this is that $\partial_\alpha B(\alpha_0, \alpha)$ is non-singular.

In general, only for $m = 1$ the QBE determine all (i.e., *both*) branches through (u_0, λ_0). In this case, (13) reduces to

$$a\alpha_1^2 + 2b\alpha_1\alpha_0 + c\alpha_0^2 = 0, \quad a = a_{111},\ b = b_{11},\ c = c_1, \tag{14}$$

and if (α_0, α_1) is one solution, then the other is distinct (linear independent) if $a\alpha_1 + b\alpha_0 \neq 0$. For the branch switching, let (α_0, α_1) with $\alpha_0 = \lambda_0'$ and $\alpha_1 = \psi^T\dot{u}_0$ be determined by the branch already computed, and, assuming the generic case $\alpha_0 \neq 0$, let $\phi_0 = \frac{1}{\alpha_0}(u_0' - \alpha_1\phi_1)$. Then the other root of (14) is $(\overline{\alpha}_0, \overline{\alpha}_1)$ with $\dfrac{\overline{\alpha}_1}{\overline{\alpha}_0} = -\left(\dfrac{\alpha_1}{\alpha_0} + \dfrac{2b}{a}\right)$, and the tangent to the bifurcating branch is $\tau_1 = (\overline{\alpha}_1\phi_1 + \overline{\alpha}_0\phi_0, \overline{\alpha}_0)$. For normalization we choose $\overline{\alpha}_0 = a$, and thus obtain the algorithm `swibra`, see [UWR14, §2.2], and Algorithm 2.1.

Algorithm 2.1: Branch-switching at a simple bifurcation points via `p=swibra(dir,ptnr,newdir)`, and subsequent continuation of the new branch by `p=cont(p)`. Here the arguments `dir, ptnr` stand for the `pde2path` setting that the branch point has filename `ptnr.mat` in directory `dir`, `p` is used as the name of the `pde2path` matlab struct which stores the problem data, with several substructs such as `p.mat` (see also Algorithm 2.2), and `newdir` is the new directory to store continuation results. The main `pde2path` continuation routine `cont` implements (8) and the associated postprocessing such as bifurcation detection and localization and so on.

1. Compute ϕ_1, ψ_1 with $G_u^0\phi_1 = 0, {G_u^0}^T\psi_1 = 0$, $\|\phi_1\| = 1$, $\langle\psi_1, \phi_1\rangle = 1$, let $\alpha_0 = \lambda_0'$, $\alpha_1 = \psi^T u_0'$, $\phi_0 = \alpha_0^{-1}(u_0' - \alpha_1\phi_1)$, with (λ_0', u_0') from the branch already computed, and compute a, b, c from (14) (see also Remark 2.1).
   If $\alpha_0 \neq 0$, set $\overline{\alpha}_1 = -\left(\frac{a\alpha_1}{\alpha_0} + 2b\right)$ and $\tau_1 = \begin{pmatrix}\overline{\alpha}_1\phi_1 + a\phi_0 \\ a\end{pmatrix}$.
   If $\alpha_0 = 0$, then choose $\tau = \begin{pmatrix}0 \\ \mathrm{ds}\end{pmatrix}$ as a guess for the bifurcation direction (horizontal branch).
   Choose a weight ξ and a stepsize ds, and normalize $\tau_0 = \tau_1/\|\tau_1\|_\xi$.
2. Use `p=cont(p)` to continue the new branch.

2.3 An algorithm for branch switching at multiple bifurcation points

The case $m \geq 2$ is more difficult, and the QBE (13) may (and typically will) not yield all bifurcating branches. The question which order of Taylor expansion in the sense of (13) is needed is called determinacy. In a loose sense, see [Mei00, §6.4] for precise definitions, a given system of algebraic bifurcations equations in α (such as (13)) is called k–determined if any small perturbation of order $k+1$ does not qualitatively change the set of (small) solutions. In this sense, transcritical bifurcations are (generically, i.e., unless some special structure occurs) 2–determined, and pitchfork bifurcations are generically 3–determined. Thus, to compute the α for pitchfork branches with $\alpha_0 = 0$ we need to at least consider the associated cubic bifurcation equations. In principle, in case of higher order indeterminacies, this must be further continued to higher order, which quickly becomes rather complicated. See, e.g., [Mei00, §6.7] for further discussion and a general algorithm.

Here we take a practical approach and proceed as follows. The function `qswibra` searches for solutions (α_0, α) of the QBE (13) with $\alpha_0 \neq 0$ (transcritical bifurcations). All solutions found are stored in `p.mat.qtau`, and additionally, an orthonormal base of the kernel is stored in `p.mat.ker`, where as in Algorithm 2.1 `p` is used as the name of the `pde2path` matlab struct which stores the problem data. Subsequently, we can either select (via `seltau`) a bifurcating direction from `p.mat.qtau`, or generate (via `gentau`) a guess for a bifurcating direction as a linear combination of `p.mat.ker`. Afterwards call `cont`.

Similarly, `cswibra` searches for solutions (β, α) of the cubic bifurcation equations (CBE) for pitchforks. To derive these we assume that $\lambda'(0) = 0$ for the bifurcating branch, and make the ansatz

$$u(s) = s\sum_{i=1}^{m}\alpha_i\phi_i + s^2 w, \quad \lambda(s) = \beta s^2, \tag{15}$$

with unknowns $\alpha \in \mathbb{R}^m$, $\beta \in \mathbb{R}$ and $w \in N(G_u)^\perp = \mathrm{span}\{\phi_1, \ldots, \phi_m\}^\perp$, i.e. $\langle\psi_i, w\rangle = 0, i = 1, \ldots, m$. As before, taking 2nd derivatives in s yields

$$0 = G_{uu}[u', u'] + G_u u'' + 2\lambda' G_{u\lambda}u' + G_{\lambda\lambda}\lambda'^2 + G_\lambda\lambda'',$$

and evaluating at $s = 0$ and using that $\lambda'(0) = 0$, $\lambda''(0) = 2\beta$, and $u''(0) = 2w$, we obtain

$$w = \sum_{j,k=1}^{m}\alpha_j\alpha_k\nu_{jk} + \beta\chi, \quad \nu_{jk} = -\frac{1}{2}P(G_u^{-1}G_{uu}[\phi_j, \phi_k]), \quad \chi = -\beta P(G_u^{-1}G_\lambda), \tag{16}$$

where P is the projection onto $N(G_u)^\perp$. Then taking third derivatives in s and evaluating at $s=0$, again using that $\lambda'(0)=0$, yields

$$0 = G_{uuu}[u',u',u'] + 6\beta G_{u,\lambda}u' + 6G_{uu}[u',w] + G_u u''' + G_\lambda \lambda'''. \tag{17}$$

From $G_u u''' + G_\lambda \in R(G_u)$ and projection onto ϕ_i we obtain the CBE

$$\begin{aligned}
&C(\alpha,\beta) = 0 \in \mathbb{R}^m, \qquad (18)\\
&C_i(\alpha,\beta) = \sum_{j,k,l=1}^{m} (d_{ijkl}+e_{ijkl})\alpha_j\alpha_k\alpha_l + 6\beta\sum_{j=1}^{m}(f_{ij}+g_{ij})\alpha_j, \quad i=1,\dots,m,\\
&d_{ijkl} = \langle \psi_i, G_{uuu}[\phi_j,\phi_k,\phi_l]\rangle\,, \quad e_{ijkl} = \langle \psi_i, G_{uu}[\phi_j,\nu_{kl}]\rangle\,, \quad f_{ij} = \langle \psi_i, G_{u\lambda}\phi_j\rangle\,, \quad g_{ij} = \langle \psi_i, G_{uu}[\phi_j,\chi]\rangle\,.
\end{aligned}$$

As already said, the case $m \geq 2$ is typically associated to symmetries of the underlying PDE, in which case often some additional information about the branching behaviour at a multiple bifurcation point is available, e.g., that branches are (generically) 2–or 3–determined. In that case we may expect to find all branches by suitably solving (13) and (18), see Remark 2.1. Moreover, the symmetries often yield that the number of bifurcating branches is significantly larger than m (the dimension of the kernel), but many 'different' branches are related by symmetry. For instance, for the Swift–Hohenberg (SH) equation on a so called simple cubic lattice (see §3.2), $m=3$ at the primary bifurcation from the trivial solution, but 15 different branches bifurcate, which however fall into 3 isotropy groups, i.e., lamellas, tubes, and rhombs. Thus, after solving the QBE or CBE (for linear independent coefficients (α_0,α) and (β,α), respectively), we plot the bifurcation directions, and the user should inspect these and select suitable ones.

However, in §3 and §4 we also give "natural" examples of pitchforks which are *not* 3-determined. In the first example, they arise only at special secondary parameter values of the SH equation (and hence are non-generic), but in the second example they are forced by symmetries of the domain. Partly for the case of such higher order indeterminacies we provide the function `gentau`, where the user can compose guesses for bifurcation directions 'by hand'.

Altogether, the approach is summarized in Algorithm 2.2. It is only theoretically sound for 2-determined branches and 3-determined pitchforks, but it works well and robustly for all the pattern-forming systems and related problems we considered so far.

Remark 2.1. (a) For the detection and localization of multiple BPs we use the `bifcheck=2` setting of `pde2path` (see [Uec18a, §2]), based on computing small eigenvalues of the linearizations G_u by inverse vector iteration. To determine m we identify all eigenvalues μ with $|\mu|<\mu_2$ as zero, where μ_2=`p.nc.mu2` is a user chosen constant (with default $\mu_2=10^{-3}$). If $m=1$ is detected in `q(c)swibra`, then we immediately call `swibra`. In all our examples there is a clear gap between 'zero' and 'nonzero' eigenvalues, but the user may also pass m to `q(c)swibra`, see [Uec18b].
(b) To approximate the coefficients a_{ijk}, b_{ij} and c_i for the QBE we use finite differences for the directional second derivatives in (13), i.e., for small $\delta>0$,

$$\begin{aligned}
a_{ijk} &= \frac{1}{\delta}\psi_i^T\big[G_u(u_0{+}\delta\phi_j,\lambda_0) - G_u^0\big]\phi_k,\\
b_{ij} &= \frac{1}{\delta}\psi_i^T\Big[\big[G_u(u_0{+}\delta\phi_j,\lambda_0) - G_u^0\big]\phi_0 + G_\lambda(u_0{+}\delta\phi_j,\lambda_0) - G_\lambda^0\Big],\\
c_i &= \frac{1}{\delta}\psi_i^T\Big[\big[G_u(u_0{+}\delta\phi_0,\lambda_0){-}G_u^0\big]\phi_0 + 2\big[G_\lambda(u_0{+}\delta\phi_0,\lambda_0){-}G_\lambda^0\big] + \big[G_\lambda(u_0,\lambda_0{+}\delta){-}G_\lambda^0\big]\Big].
\end{aligned} \tag{19}$$

Similarly, to approximate the third derivatives $G_{uuu}[\phi_j,\phi_k,\phi_l]$ for the CBE we use

$$\begin{aligned}
G_{uuu}[\phi_j,\phi_k,\phi_l] = \frac{1}{4\delta^2}\Big(&G_u(u_0+\delta(\phi_j+\phi_k) - G_u(u_0+\delta(\phi_j-\phi_k)\\
&- G_u(u_0+\delta(-\phi_j+\phi_k) + G_u(u_0-\delta(\phi_j+\phi_k)\Big)\phi_l,
\end{aligned} \tag{20}$$

Algorithm 2.2: `qswibra, cswibra`, and subsequent `seltau, gentau` for branch-switching at multiple bifurcation points, then `cont`. Same meaning of arguments `dir, ptnr, p0, p, newdir` as in Algorithm 2.1.

1. Call `p0=qswibra(dir,ptnr)` to find nontrivial solutions of the QBE (13); store these in `p.mat.qtau`. Additionally, store a base of $N(G_u^0)$ in `p.mat.ker`.

2a. If 1 yields nontrivial solutions of the QBE: use `p=seltau(p0,nr,newdir,2)` to choose tangent `nr` as a predictor to the new branch.

2b. Use `p=cont(p)` to continue the new branch, return to 2a to follow more branches.

3. Subsequently/alternatively (if the absence of transcritical branches is known) to 1,2, call `p0=cswibra(dir,ptnr)` to find nontrivial solutions of the CBE (18). The tangents are then stored in `p.mat.ctau`, and 'effective' predictors (u, λ) are computed from (15) with $s =$ `ds`, normalized and stored in `p.mat.pred`.

4. Proceed as in 2, i.e.: Call `p=seltau(p0,nr,newdir,3)` for choosing tangent `nr` as predictor, or `p=seltau(p0,nr,newdir,4)` to choose the quadratic predictor `nr`. Afterwards call `p=cont(p)`.

5. For (possible) branches additional to those found in 1.–4.: use `p=gentau(p0,gamma)` to generate guesses for tangents to new branches according to $\tau = \sum_i \gamma_i$ `p.mat.ker`(i), where the sum runs from 1 to `length(gamma)`. Afterwards call `p=cont(p)`.

6. If `cont` fails after branch-switching, try, e.g., different `ds` (for the quadratic predictor `p=seltau(p0,nr,4)` this theoretically requires a new call to `cswibra`).

i.e., central finite differences, which turned out to be more robust for the third derivatives than forward differences as in (19).

(c) In (16) we need to solve $m^2 + 1$ linear systems of the form $G_u v = b$; for this we naturally use the `pde2path` linear system solver already used in `cont`, or some custom solvers. The choices include, e.g., direct solvers based on a LU factorization of G_u, or, for large n, preconditioned iterative solvers based on `ilupack` [Bol11]. In our applications, n typically ranges between 10^4 and 10^5, and also for the latter (and $m = 2, 3$ and similar) the computation of the coefficients for the CBE is only a matter of seconds.

(d) To solve the QBE (13), we fix α_0 and use a Newton method (`fsolve`) with a number of initial guesses for α, by default all tuples $\alpha = (\alpha_1, \ldots, \alpha_m)$ with $\alpha_j \in \{0, 1, -1\}$. To add flexibility, the user can give a tuple $\vec{\alpha}_{0,j}$ of α_0 values. Theoretically, we could fix $\alpha_0 = 1$ if we knew 'good' initial guesses for α, but since we do not know these in general, varying α_0 has turned out to be an efficient way to scale the initial guesses for α. Two further parameters for `qswibra` (and `cswibra`) which for some cases need to be modified are `soltol` (default 10^{-20}) and `isotol` (default 10^{-10}), where α is taken as a solution if $\|B(\alpha_0, \alpha)\| <$ `soltol`, and taken to be isolated if $|\det \partial_\alpha B(\alpha_0, \alpha)| >$ `isotol`. In any case, the solvers for the QBE (13) and the CBE (18) are not guaranteed to find all solutions, which besides possible high order indeterminacy is another reason why we provide `gentau`.

(e) To solve the CBE (18), we similarly use a Newton method with initial guesses for α, and additionally loop over $\beta \in \{\pm\beta_0, \pm\beta_0/10\}$, with $\beta_0 = 0.01$ by default. Again, theoretically $\beta = \pm 1$ would be sufficient, and different β only scale the solutions α, but the behaviour of the Newton loops depends on β, i.e., β implicitly scales the initial guesses. Once a solution α (isolated, and linearly independent of each previous solution) has been found, the value of β plays no role for the tangent $\tau = (\sum_{i=1}^m \alpha_i \phi_i, 0)$, which we then normalize. Additionally, we store the normalized quadratic predictors ('effective tangents') (u, λ) computed from (15) with $s =$ `ds` in `p.mat.pred`. However, only in rare cases do these effective tangents seem superior to the tangents in the sense that they yield faster convergence of initial Newton loops, and we recommend to generically use the tangents.

(f) An alternative to the splitting `q(c)swibra, seltau` and then `cont` on the full (discretized) system is described in [Mei00, §6.7], where extensions of the QBE and CBE or even higher order versions are used to actually compute the bifurcating branch.

(g) To combine the calls to `qswibra` and `cswibra` we provide the (convenience) call `qcswibra`. This slightly reduces the overhead, but our experience is that the separate calls to `qswibra` and `cswibra` give a clearer code and understanding. ⌋

3 Example: Pattern formation in the Swift-Hohenberg equation

As our main example we consider the (quadratic-cubic) Swift-Hohenberg (SH) equation

$$\partial_t u = -(1+\Delta)^2 u + \lambda u + \nu u^2 - u^3, \quad u = u(x,t) \in \mathbb{R},\ t \geq 0,\ x \in \Omega, \tag{21}$$

where $\Omega \subset \mathbb{R}^d$, is a bounded domain, $d = 1, 2, 3$ (1D, 2D and 3D cases, respectively), with instability parameter $\lambda \in \mathbb{R}$, second parameter $\nu \in \mathbb{R}$, and boundary conditions (BC) $\partial_n u|_{\partial\Omega} = \partial_n(\Delta u)|_{\partial\Omega} = 0$. This is *not* a RD system, i.e., not of class (1), but a canonical model problem for bifurcations and pattern formation in dissipative system [CH93, Pis06, SU17]. See §4 for further remarks. The original (cubic) SH model [SH77] corresponds to $\nu = 0$, while the case $f(u) = \nu u^3 - u^5$ instead of $f(u) = \nu u^2 - u^3$ is called the cubic-quintic SH equation. For validation of Algorithm 2.2 we review some theory for (21) and pattern formation in general, but no problem specific analytical results are used in the numerics. For speed and ease of presentation we choose rather small domains which accomodate the primary bifurcations, but this is not crucial in the sense that general domains (with the same symmetries) give the same bifurcations with possibly a slightly different wave number.

For all $\lambda \in \mathbb{R}$, (21) has the spatially homogenous state $u^* \equiv 0$ (trivial branch). Over $\mathbb{R}^d$, the linearization $\partial_t v = -(1+\Delta)^2 v + \lambda v$ at $u^* \equiv 0$ has the solutions $v(x,t) = \mathrm{e}^{\mathrm{i}k\cdot x + \mu(k,\lambda)t}$, $k \in \mathbb{R}^d$, where

$$\mu(k,\lambda) = -(1-|k|^2)^2 + \lambda, \quad |k|^2 := k_1^2 + \ldots + k_d^2. \tag{22}$$

Thus, $u^* \equiv 0$ is asymptotically stable for $\lambda < 0$, unstable for $\lambda > 0$ with respect to periodic waves with wave vector k with $|k| = k_c = 1$, and for bounded $\Omega \subset \mathbb{R}$ we expect a simple pitchfork bifurcation of spatially 2π periodic patterns at $\lambda = 0$, if permitted by the domain and the BC. In 2D and 3D, i.e., bounded $\Omega \subset \mathbb{R}^d$, $d = 2, 3$, depending on the symmetries of Ω, this primary bifurcation may be double (stripes and spots in 2D) or triple (lamellas, tubes and rhombs on SC lattices in 3D), or of even higher multiplicity (for, e.g., BCC and FCC lattices), see [CK97]). The `pde2path` demo directory `demos/sh`, included in the `pde2path` download, deals with the double and triple cases, and illustrates a few other aspects such as rewriting the SH equation as a second order system in a consistent way, and secondary bifurcations and localized patterns, see [Uec18b].

Remark 3.1. (a) Since (21) has the equivariance $(u,\nu) \mapsto (-u,-\nu)$ we can restrict to $\nu \geq 0$.
(b) Some indeterminacies of 2D problems often follow from symmetry considerations. For instance, if the problem has the dihedral group D_j (generated by reflections in x, say, and rotation by $2\pi/j$) as a symmetry group, and if G_u has a two dimensional kernel that is invariant and irreducible under D_j, then it is known that the bifurcation equations are not k–determined for $k < j-1$. This follows from, e.g., [GS02, Theorem 2.24]. ⌋

3.1 2D

Square domains. We first consider the square domain $\Omega = (-2\pi, 2\pi)^2$, with coordinates (x,y), and focus on the first BP at $(u,\lambda) = (0,0)$. The linearization has the two–dimensional kernel spanned by $\cos(x)$ and $\cos(y)$, which is invariant under the action of D_4. Thus, by Remark 3.1 the problem is at best 3-determined. Analytically, the problem is best understood via the pertinent amplitude equations. For these we make the ansatz

$$u = \varepsilon(A_1 e_{1,0} + A_2 e_{0,1}) + \text{h.o.t} + \text{c.c.}, \quad \lambda = \varepsilon^2\mu,\ \mu = \pm 1, \tag{23}$$

where $0 < \varepsilon \ll 1$ is an amplitude parameter, the A_j are (complex) amplitudes depending on a slow time $T = \varepsilon^2 t$, $e_{k_1,k_2} = \mathrm{e}^{\mathrm{i}(k_1 x + k_2 y)}$, c.c. denotes the complex conjugate of the preceeding terms, and h.o.t

stands for higher order (in amplitude ε) terms. For Neumann BC the A_j are real, but the calculus is most easy if we use complex notation and relations such as $e_{k_1,k_2}^2 = e_{2k_1,2k_2}$ and so on. Plugging (23) into (21), first solving for $\mathcal{O}(\varepsilon^2)$ terms at $e_{0,0}, e_{2,0}, e_{1,1}$ and $e_{0,2}$, and then collecting $\mathcal{O}(\varepsilon^3)$ terms at $e_{1,0}$ and $e_{0,1}$ (see [Uec18b] for details) yields the amplitude equations

$$\frac{d}{dT}\begin{pmatrix} A_1 \\ A_2 \end{pmatrix} = \begin{pmatrix} A_1(\mu - c_1|A_1|^2 - c_2|A_2|^2) \\ A_2(\mu - c_1|A_2|^2 - c_2|A_1|^2) \end{pmatrix}, \quad c_1 = 3 - \frac{38}{9}\nu^2, \quad c_2 = 6 - 12\nu^2. \tag{24}$$

These amplitude equations (truncated at third order) are essentially a different version of the CBE (18). For the bifurcations from a homogeneous solution $u \equiv u_0$ on a square with two dimensional kernel, they *always* take the form (24), see [Erm91, GS02] and [Hoy06, §4.3.1, §5.3], and the specifics of the system condense in the coefficients c_1, c_2. The problem is 3-determined except if $c_1 = 0$ or $|c_1| = |c_2|$. If $c_2 = c_1$, then, returning to real notation $A_{1,2} \in \mathbb{R}$ and without loss of generality assuming that $\mu, c_1 > 0$, we have a circle $A_1^2 + A_2^2 = \mu/c_1$ of nontrivial solutions. For $c_2 = -c_1$, we have 'vertical branches' of spots $\mu = 0$ and $(A_1, A_2) = s(1, \pm 1)$, $s \in \mathbb{R}$, and for $c_1 = 0$ we have vertical branches $\mu = 0$ of stripes $(A_1, A_2) = s(0, 1), (A_1, A_2) = s(1, 0), s \in \mathbb{R}$. In all these cases, the bifurcating branches would be determined at fifth order.

Our particular problem (24) at the first BP is thus 3-determined except if $\nu \in \{\nu_1, \nu_2, \nu_3\}$, where

$$\nu_1 := \sqrt{\frac{27}{70}} \ (c_1 = c_2 > 0), \quad \nu_2 := \sqrt{\frac{81}{146}} \ (c_1 = -c_2 > 0), \quad \nu_3 = \sqrt{\frac{27}{38}} \ (c_1 = 0).$$

For $\nu \notin \{\nu_1, \nu_2, \nu_3\}$ we have the nontrivial solutions

$$A_1 = A_2 = \pm\sqrt{\mu/(c_1 + c_2)} \text{ (spots)}, \ A_1 = \pm\sqrt{\mu/c_1}, A_2 = 0 \text{ (or } A_1, A_2 \text{ interchanged, stripes)}, \tag{25}$$

where we assume the right sign of μ for the respective solutions to exist (sub-or supercritically). Moreover, also the stability of these nontrivial solutions can immediately be evaluated, see [Erm91, Theorem], [Hoy06, Fig. 4.10].

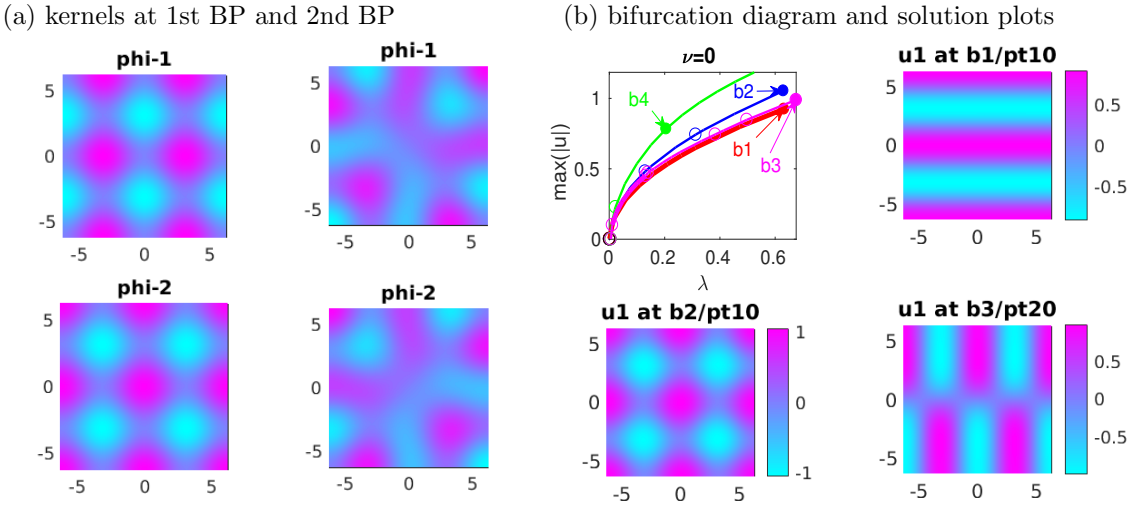

Figure 1: (a) Numerical kernel vectors for (21) at the first (left column) and second (right column) BP on the square $\Omega = (-2\pi, 2\pi)^2$. `cswibra` automatically generates the bifurcation directions from these kernel vectors, and (b) shows the bifurcation diagram and selected solutions. The green branch corresponds to planform ϕ_1 at the second BP. There are secondary BPs on all branches except on the stripes `b1` from the 1st BP, which are stable throughout, and the magenta branch `b3` is stable for λ between 0.01 and 0.13.

Figure 1(a) shows the kernel vectors obtained numerically (via inverse vector iteration in `eigs`) at $(u, \lambda) = (0, 0)$ and at the second BP $(u, \lambda) = (0, 1/16^2)$. We discretized $\Omega = (-\pi, \pi)^2$ with 4802 triangles, and the 6 smallest eigenvalues of $G_u(0, 0)$ are

$$-6.85 \times 10^{-7}, \ -6.0583 \times 10^{-7}, \ 0.00477, \ 0.00479, \ 0.0183, \ 0.03274,$$

from which `cswibra` directly identifies $m = 2$ at $\lambda = 0$, and similar at $\lambda = 1/16^2$, while the third BP is simple (analytically corresponding to $k = (3/4, 3/4)$ and hence $\lambda = 1/64$). The computed eigenvectors at $\lambda = 0$ are spots instead of the two 'natural' stripe modes $\cos(x), \cos(y)$, although it is rather easy to see how to obtain stripes from ϕ_1, ϕ_2, namely $\cos(x) \sim \phi_1 - \phi_2$ and $\cos(y) \sim \phi_1 + \phi_2$, and similarly, e.g., $\cos(x)\cos(y/4) \sim -(\phi_1 + \phi_2)$ at $\lambda = 1/16^2$. However, this may not be obvious in general, and for $\nu \notin \{\nu_1, \nu_2, \nu_3\}$ the easiest way to obtain the bifurcation directions is to call `cswibra`, where moreover the coefficients α of the tangents do not depend on ν, i.e., only $\lambda''(0)$ and the quadratic correction w do. Figure 1 (b) shows the bifurcation diagram of four branches bifurcating at the first two BPs, two at each. The three solution plots show that the branches follow the planforms determined at branch switching from the trivial branch. The green branch `b4` (solution plot omitted) is of type ϕ_1 from the 2nd BP.

For $\nu \in \{\nu_1, \nu_2, \nu_3\}$, or more precisely, e.g., $|\nu - \nu_1| < \delta_0 \approx 0.005$ in the default setting of `cswibra`[2], `cswibra` correctly returns that the problem is not 3-determined because non–isolated solutions α of the CBE are found. Since in this problem the tangents do not depend on ν, a simple trick to proceed is to use α values obtained at some other ν.

Rectangular domains with hexagonal dual grids. A special situation occurs for problems with quadratic terms over domains which allow resonant wave vector triads, i.e., critical wave vectors $k^{(1)}, k^{(2)}$ and $k^{(3)}$, $|k^{(j)}| = k_c = 1$ such that any $k^{(j)}$ is a linear combination of the other two. As these lie on the circle $|k| = k_c$, the angle between them is $2\pi/3$, and on a rectangular domain this is compatible with the BC for $\Omega = (-l_1\pi, l_1\pi) \times (-l_2\pi/\sqrt{3}, l_2\pi/\sqrt{3})$, such that $\mu_1 = 0$ at $\lambda = 0$ is double with $k^{(1)} = (1, 0)$, $\phi_1 = \cos(x)$, $k^{(2)} = (-1/2, \sqrt{3}/2)$, and $k^{(3)} = -(1/2, \sqrt{3}/2)$, and, e.g., $\phi_2(x, y) = e_2 + e_3 = \cos(x/2)\cos(\sqrt{3}y/2)$,

The ansatz

$$u(x,t) = A_1(t)e_1 + A_2(t)e_2(t) + A_3(t)e_3 + \text{h.o.t} \tag{26}$$

and the pertinent symmetry considerations then yield the amplitude equations (in complex notation, although again for Neumann BC the A_j are real, and, moreover $A_3 = A_2$), truncated at third order,

$$\begin{aligned}
\dot{A}_1 &= \mu A_1 + \gamma\overline{A_2 A_3} - c_1|A_1|^2 A_1 - c_2(|A_2|^2 + |A_3|^2)A_1,\\
\dot{A}_2 &= \mu A_2 + \gamma\overline{A_1 A_3} - c_1|A_2|^2 A_3 - c_2(|A_1|^2 + |A_3|^2)A_2,\\
\dot{A}_3 &= \mu A_3 + \gamma\overline{A_1 A_2} - c_1|A_3|^2 A_3 - c_2(|A_1|^2 + |A_2|^2)A_3,
\end{aligned} \tag{27}$$

$\mu = \lambda$. The ε–scaling from (23) is omitted in (26) because the derivation of (27) assumes that the quadratic terms in the original system are small (and in particular $\gamma = 0$ if the quadratic terms vanish, i.e., if the original system has the symmetry $u \mapsto -u$). For (21) with $f(u) = \nu u^2 - u^3$ we obtain (recalling that we treat $|\nu|$ as small)

$$\gamma = 2\nu + \mathcal{O}(|\lambda\nu|), \quad c_1 = 3 + \mathcal{O}(|\lambda| + \nu^2), \quad c_2 = 6 + \mathcal{O}(|\lambda| + \nu^2). \tag{28}$$

The problem has similar (non-generic) indeterminacies as (24), but is generically 3-determined, and for ν=0 we have we have three bifurcating branches: *Stripes* (str) $A_1 = \pm\sqrt{\mu/c_1}$, $A_2 = A_3 = 0$, *hexagons* (hex) $A_1 = A_2 = A_3 = A$, $A = \frac{\gamma}{2(c_1+2c_2)} \pm \sqrt{\frac{\gamma^2}{4(c_1+2c_2)^2} + \frac{\mu}{c_1+2c_2}}$, and *pathwork quilts* (pq) $A_1 = 0$, $A_2 = A_3 = \pm\sqrt{\frac{\mu}{c_1+c_2}}$ (*only* if $\gamma = 0$). For $\gamma = 2\nu + \text{h.o.t} \neq 0$, the hexagons bifurcate transcritically, i.e., the hex branch is then 2-determined, and the pq branch comes from secondary bifurcations. Thus, for the case $\nu = 0$ we use `cswibra` to obtain the three bifurcating branches str, hex, and pq, while for $\nu \neq 0$ we obtain the hex branch from `qswibra`. This works out of the box with default numerical settings, see Fig. 2 and [Uec18b].

[2] δ_0 decreases with `isotol`, where $|\det \partial_\alpha C(\alpha, \beta)| >$ `isotol` is the criterion used to classify solutions α as isolated

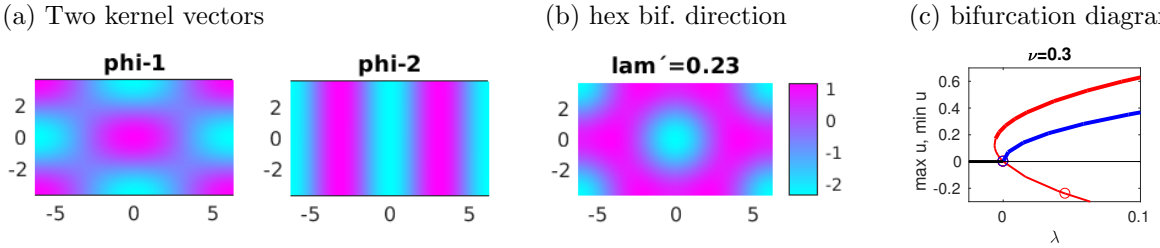

Figure 2: Selected results from demo `sh/cmds2dhex` for (21) over $\Omega=(-2\pi,2\pi)\times(-2\pi/\sqrt{3},2\pi/\sqrt{3})$. (a) The two numerical kernel vectors at $(u,\lambda)=(0,0)$. (b) hex-bifurcation direction obtained from `qswibra` for $\nu=0.3$. Since $\phi_{1,2}$ in (a) correspond to patchwork-quilt and stripe modes, here clearly the hex direction comes from (roughly) equal amplitude superposition. The values in (b) are $\alpha=(-0.0317,0.0224)$ for $\alpha_0=0.001$, and $\lambda'=0.23$ in the title comes from the normalization of $\tau=(u'(0),\lambda'(0))$ (which depends on the weight ξ in (7)). (c) Bifurcation diagram of stripes (blue) and hexagons (red), for which we plot $\min u$ for the 'gap' leg bifurcating to the right.

3.2 A small cube as a model for the SC lattice

The bifurcations of Turing patterns in 3D are in general rather complicated, and so far mostly the primary bifurcations have been analyzed to some extent [CK97, CK99, CK01]. Here we restrict to a simple 3D analogon of the square domain, namely $\Omega=(-\pi,\pi)^3$ with Neumann BC $\partial_n u=\partial_n\Delta u=0$ on $\partial\Omega$, which corresponds to a so called simple cube (SC) (critical) wave vector lattice. At the first bifurcation point $\lambda=0$ we have a three dimensional kernel spanned for instance by three lammellas, i.e., $N(G_u)=\mathrm{span}\{\cos(x),\cos(y),\cos(z)\}$. The ansatz $\lambda=\mu\varepsilon^2$, $0<\varepsilon\ll 1,\mu=\pm1$, and

$$u=\varepsilon(A_1e_{100}+A_2e_{010}+A_3e_{001})+\text{h.o.t}+\text{c.c.},\quad e_k=\mathrm{e}^{\mathrm{i}k\cdot x},\tag{29}$$

yields the amplitude equations

$$\frac{d}{dT}\begin{pmatrix}A_1\\A_2\\A_3\end{pmatrix}=\begin{pmatrix}A_1(\mu-c_1|A_1|^2-c_2(|A_2|^2+|A_3|^2))\\A_2(\mu-c_1|A_2|^2-c_2(|A_1|^2+|A_3|^2))\\A_3(\mu-c_1|A_3|^2-c_2(|A_2|^2+|A_3|^2))\end{pmatrix},\tag{30}$$

where again $c_1=3-\frac{38}{9}\nu^2$ and $c_2=6-12\nu^2$. Naturally, this contains the system (24) as a subsystem with $A_3=0$ (or $A_1=0$ or $A_2=0$), and the stripes and spots of the 2D problem are now classified as *lamellas* $A_1=\pm\sqrt{\mu/c_1}, A_2{=}A_3{=}0$, *tubes* $A_1=A_2=\pm\sqrt{\mu/(c_1+c_2)}, A_3=0$, respectively, where clearly A_1,A_2,A_3 can be permuted, giving different orientations of the lamellas and tubes. Additionally we have the *rhombs* $A_1=A_2=A_3=\pm\sqrt{\mu/(c_1+2c_2)}$, where again depending on c_1,c_2 we assume the right sign of μ.

Moreover, (30) is 3–determined except if $c_1=0,|c_1|=|c_2|$, and additionally if $|c_1|=2|c_2|$. For $c_1=0,|c_1|=|c_2|$ we have non-isolated solutions as above with $A_3=0$. For $c_1=2c_2$ we have the sphere $A_1^2+A_2^2+A_3^2=\mu/c_1$ of non-isolated solutions, and for $c_1=-2c_2$ we have vertical branches $\mu=0$, $(A_1,A_2,A_3)=s(1,\pm1,\pm1)$, $s\in\mathbb{R}$, of rhombs. The additional exceptional values of ν are $\nu_4=\sqrt{\frac{81}{178}}$ $(c_1=2c_2)$ and $\nu_5=\sqrt{\frac{243}{252}}$ $(c_1=-2c_2)$. Again, the stabilities of the nontrivial branches on the amplitude equations level can efficiently be computed using symmetry, see, e.g., [CK99], which inter alia yields that the tubes are always unstable close to bifurcation, and either the rhombs or the lamellas can be stable, but not both, see also [AGH$^+$05, Theorem 1].

Similarly to the 2D case of a square, from the amplitude equations (30), we know that all bifurcations at $\lambda=0$ (and in fact at all subsequent bifurcation points) must be pitchforks, and thus for $\nu\notin\{\nu_1,\dots,\nu_5\}$ we directly use `cswibra` to obtain the bifurcation directions. Figure 3 shows some results. In (a) we give the three numerically obtained kernel vectors ϕ_1,ϕ_2,ϕ_3, which look like distorted lamellas, and it is not entirely obvious how to compose the pertinent three (modulo symmetries) bifurcation directions from ϕ_1,ϕ_2,ϕ_3. However, calling `cswibra` (with a significantly smaller `isotol` $=10^{-16}$ to account for the three small eigenvalues of $\partial_\alpha C(\beta,\alpha)\in\mathbb{R}^{3\times3}$) yields eight bifurcation directions, of which we plot three, one of each isotropy subgroup (equivalent branches under

rotation and translation), i.e., τ_1, τ_2, τ_3 in (b). Finally, (c) shows the (partial) bifurcation diagrams for $\nu = 0$ (all branches supercritical, with the lamellas stable), and $\nu = 1.2$ (all branches subcritical).

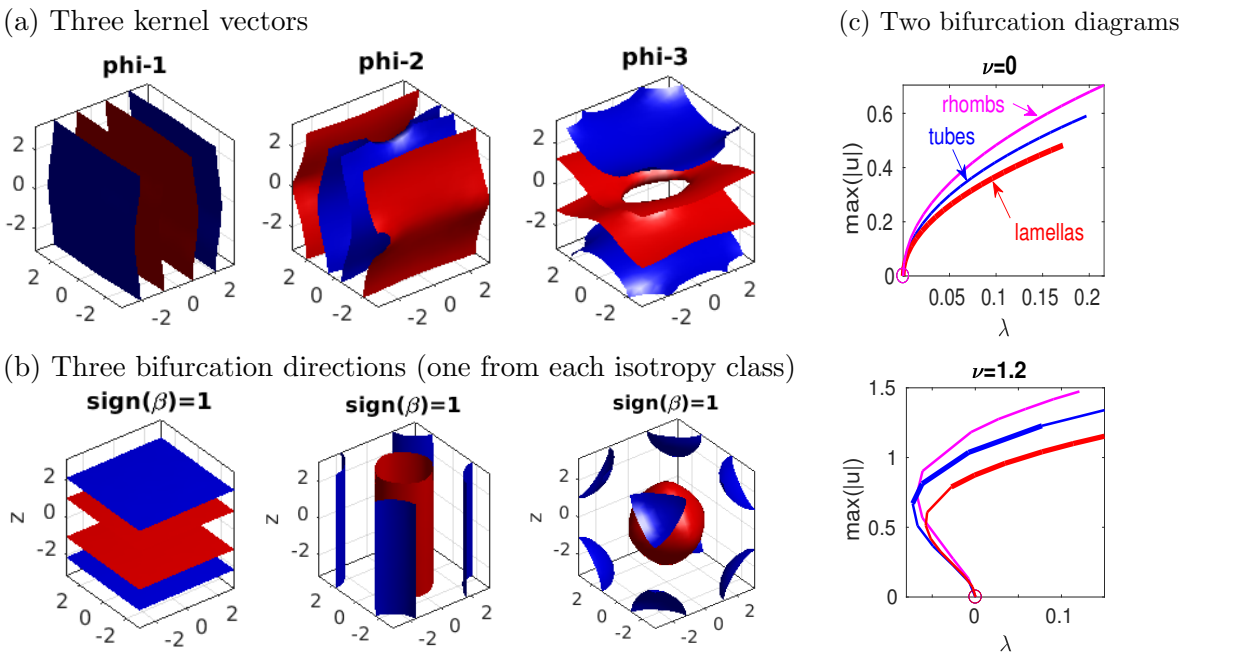

Figure 3: Selected results from demo `sh/cmds3dcube`. Primary bifurcations at $\lambda = 0$ in (21) over the cube $\Omega = (-\pi, \pi)^3$ with homogeneous Neumann BC, discretized by 34992 tetrahedral elements. (a) Isosurface plot of u for the kernel vectors obtained from `eigs`, where blue and red correspond to $m_{\rm blue} = \frac{3}{4}m_0 + \frac{1}{4}m_1$, $m_{\rm red} = \frac{1}{4}m_0 + \frac{3}{4}m_1$, respectively, with $m_0 = \min u$, $m_1 = \max u$. (b) Three (of 8) bifurcation directions obtained from `cswibra`, with $\alpha = (0.12, -0.26, 0.93), (0.58, -0.51, -0.21), (1.6, -1.63, 0.79)$, respectively. The other five are obtained from symmetry, i.e., rotation and/or translation. `sign`$(\beta) =$ `1` refers to $\nu = 0$. (c) Bifurcation diagrams, $\nu = 0$, and $\nu = 1.2$, stable branches as thicker lines. The solutions on the branches correspomd to the planforms predicted at bifurcation.

Remark 3.2. The results from Fig. 3 are from a standard mesh obtained from a Delauney triangulation of a regular grid; the mesh therefore lacks reflection symmetry. If instead we use a criss–cross type mesh, which has slightly more symmetry, see [Uec18b, §3.1.6], then we obtain less distorted lamellas as kernel vectors in (a) (and the same results in (b) and (c)). Thus, here we deliberately chose a "poor" mesh to illustrate that this makes no difference for `cswibra`.

On the other hand, in [Uec18b] we also consider the so called body centered cubic (BCC) lattice, where similar to the hexagons in Fig. 2 a branch of "balls" (or more precisely BCCs) bifurcates transcritically. While this bifurcation is correctly computed by `qswibra` on both, standard and criss-cross meshes, the continuation of the BCC branch works much better on the latter. This shows that mesh–symmetry may play an important role in continuation. Again, see [Uec18b, §3.1.6] for further details. ⌋

4 Further demos and remarks

We revised a number of `pde2path` demos to incorporate Algorithm 2.2. For instance, the demo `schnakpat` considers 1D, 2D and 3D Turing patterns in the Schnakenberg reaction diffusion system that (in 2D) has already been considered in [UWR14, §4.2] and [UW14], where however we slightly distorted the domains to break up double bifurcation points. Using `qswibra` and `cswibra` we can now study in a clean fashion bifurcations from the homogeneous branch to stripes and hexagonal spots over 2D boxes, and additionally treat some 3D examples. See [Uec18b] for details.

Additionally, the demo `hexex` considers the example from [Mei00, §6.8.2] of the scalar PDE

$$G(u, \lambda) := \Delta u + \lambda(u + u^3) = 0 \tag{31}$$

on a hexagon Ω with unit side-lengths and Dirichlet BC $u|_{\partial\Omega} = 0$. On the trivial branch ($u \equiv 0, \lambda \in \mathbb{R}$), there is a simple bifurcation point at $\lambda = \lambda_1 \approx 7.14$, a double bifurcation point at $\lambda = \lambda_2 \approx 18$, and further bifurcations at $\lambda = \lambda_3 \approx 32.5$ (double), $\lambda = \lambda_4 \approx 37.6$ (simple), ... See Fig. 4(a) for the kernel vectors at λ_2. At the simple BPs we can use `swibra`. However, the problem is $D_6 \times Z_2$ equivariant, and thus we expect pitchfork bifurcations at the multiple bifurcation points which are at best 5-determined, cf. Remark 3.1(b). Therefore, the bifurcation directions cannot be computed with `cswibra`, which correctly reports that only non–isolated solutions α are found.

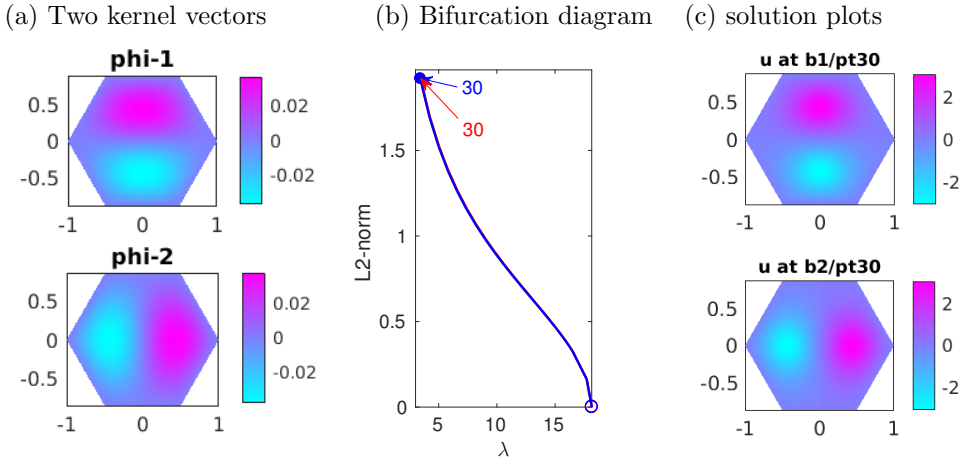

Figure 4: Results from the demo `hexex` for bifurcations at the second BP for (31).

Thus we try `gentau`, for instance with the natural choices $\gamma = (1, 0)$ and $\gamma = (0, 1)$. This turns out to immediately yield two bifurcating branches `b1, b2`, i.e., the tangents to these branches coincide with the numerical kernel vectors. Moreover, for mixed choices of γ, i.e., $\gamma = (\gamma_1, \gamma_2)$ with $\gamma_1\gamma_2 \neq 0$, if the first Newton loop converges, then the convergence is to one (isotropy class) of these two branches. In fact, this convergence occurs for a large majority of γ values, and only selected large vectors γ give non-convergence. In summary we conclude that exactly the two (classes) of distinct branches `b1, b2` bifurcate, which fully agrees with the high-order determinacy analysis in [Mei00, §6.8.2]. Thus, `gentau`, possibly with some trial and error, can be an efficient method to find all pertinent bifurcating branches of determinacy $k \geq 4$.

References

[AGH+05] M. Alber, T. Glimm, H. G. E. Hentschel, B. Kazmierczak, and S. A. Newman. Stability of n-dimensional patterns in a generalized Turing system: implications for biological pattern formation. *Nonlinearity*, 18(1):125–138, 2005.

[BGUY17] S. Bier, N. Gavish, H. Uecker, and A. Yochelis. Mean field approach to first and second order phase transitions in ionic liquids. *PRE*, 95:060201, 2017.

[Bol11] M. Bollhöfer. ILUPACK V2.4, `www.icm.tu-bs.de/~bolle/ilupack/`, 2011.

[CH93] M.C. Cross and P.C. Hohenberg. Pattern formation outside equilibrium. *Rev. Mod. Phys.*, 65:854–1190, 1993.

[CK97] T. K. Callahan and E. Knobloch. Symmetry-breaking bifurcations on cubic lattices. *Nonlinearity*, 10(5), 1997.

[CK99] T. K. Callahan and E. Knobloch. Pattern formation in three-dimensional reaction-diffusion systems. *Phys. D*, 132(3):339–362, 1999.

[CK01] T. K. Callahan and E. Knobloch. Long-wavelength instabilities of three-dimensional patterns. *Phys. Rev. E*, 64:036214, 2001.

[DCF+97] E. Doedel, A. R. Champneys, Th. F. Fairgrieve, Y. A. Kuznetsov, Bj. Sandstede, and X. Wang. AUTO: Continuation and bifurcation software for ordinary differential equations (with HomCont). `http://indy.cs.concordia.ca/auto/`, 1997.

[DGK03] A. Dhooge, W. Govaerts, and Yu.A. Kuznetsov. MATCONT: a matlab package for numerical bifurcation analysis of ODEs. *ACM Trans. Math. Software*, 29:141–164, 2003.

[Erm91] B. Ermentrout. Stripes or spots? Nonlinear effects in bifurcation of reaction-diffusion equations on the square. *Proc. R. Soc. Lond., Ser. A*, 434(1891):413–417, 1991.

[GS02] M. Golubitsky and I. Stewart. *The symmetry perspective*. Birkhäuser, Basel, 2002.

[Hoy06] R.B. Hoyle. *Pattern formation*. Cambridge University Press., 2006.

[Kel77] H.B. Keller. Numerical solution of bifurcation and nonlinear eigenvalue problems. Application of bifurcation theory, Proc. adv. Semin., Madison/Wis. 1976, 359-384, 1977.

[Kie79] H. Kielhöfer. Hopf bifurcation at multiple eigenvalues. *Arch. Rational Mech. Anal.*, 69(1):53–83, 1979.

[KL72] H. B. Keller and W. F. Langford. Iterations, perturbations and multiplicities for nonlinear bifurcation problems. *Arch. Rational Mech. Anal.*, 48:83–108, 1972.

[Kuz04] Y. A. Kuznetsov. *Elements of applied bifurcation theory. 3rd ed.* Springer, 2004.

[Mei00] Z. Mei. *Numerical bifurcation analysis for reaction-diffusion equations*. Springer, 2000.

[Mur89] J. D. Murray. *Mathematical Biology*. Springer, Berlin, 1989.

[Pis06] L.M. Pismen. *Patterns and interfaces in dissipative dynamics*. Springer, 2006.

[SH77] J. Swift and P.C. Hohenberg. Hydrodynamic fluctuations at the convective instability. *Physical Review A*, 15(1):319–328, 1977.

[SU17] G. Schneider and H. Uecker. *Nonlinear PDE – a dynamical systems approach*, volume 182 of *Graduate Studies Mathematics*. AMS, 2017.

[Tur52] A. Turing. The chemical basis of morphogenesis. *Phil. Trans. Roy. Soc. B*, 237:37–72, 1952.

[Uec16] H. Uecker. Optimal harvesting and spatial patterns in a semi arid vegetation system. *Natural Resource Modelling*, 29(2):229–258, 2016.

[Uec18a] H. Uecker. Hopf bifurcation and time periodic orbits with pde2path – algorithms and applications, *Comm. in Comp. Phys*, to appear, 2018.

[Uec18b] H. Uecker. Pattern formation with pde2path – a tutorial, 2018.

[Uec18c] H. Uecker. `www.staff.uni-oldenburg.de/hannes.uecker/pde2path`, 2018.

[UW14] H. Uecker and D. Wetzel. Numerical results for snaking of patterns over patterns in some 2D Selkov-Schnakenberg Reaction-Diffusion systems. *SIADS*, 13-1:94–128, 2014.

[UWR14] H. Uecker, D. Wetzel, and J. Rademacher. pde2path – a Matlab package for continuation and bifurcation in 2D elliptic systems. *NMTMA*, 7:58–106, 2014.

[Wet16] D. Wetzel. Pattern analysis in a benthic bacteria-nutrient system. *Math. Biosci. Eng.*, 13(2):303–332, 2016.

[ZUFM17] Y. Zelnik, H. Uecker, U. Feudel, and E. Meron. Desertification by front propagation? *Journal of Theoretical Biology*, pages 27–35, 2017.